https://doi.org/10.3311/PPee.44126
Creative Commons Attribution

Periodica Polytechnica Electrical Engineering and Computer Science

Achieving Specific Compensation of Current Harmonics in Grid Connected PV Power Station Under Limited Reactive Current

Atallah Ouai[1*]

[1] LACoSERE Laboratory, Department of Electrical Engineering, Faculty of Technology, University Amar Telidji of Laghouat, P. O. B. 37, Ghardaia Street, 03000 Laghouat, Algeria
[*] Corresponding author, e-mail: a.ouai@lagh-univ.dz

Received: 27 March 2026, Accepted: 29 June 2026, Published online: 30 October 2026

Abstract

The new control strategy presented in this paper focuses on improving the capacity of active harmonic filtering in a grid connected PV Power Station (PVPS). The PV field is connected to the grid through a PCS (Power Conditioning System: boost chopper + DC-AC PWM converter). Based on the nominal PVPS power value, reactive power and harmonic currents generated by the nonlinear load can be compensated. The proposed approach is applied to the grid-side converter to realize flexible active power injection and, at the same time, improves power quality at the CP (Connecting Point) by compensating reactive power and ensuring active filtering of the 5th and 7th harmonics without reaching the reactive current limit. To guarantee high optimal filtering results of these specific harmonics, a harmonic isolation method based on a High Selectivity Filter (HSF) is employed. This allows the electrical grid to supply only sinusoidal currents under a constant power factor. In this work, to improve the capacity of the PV inverter in terms of harmonics mitigation, it is suggested to suppress instantaneously the high-order harmonics (the 5th and 7th harmonics) if possible; otherwise, the specific compensation of current harmonics is canceled. Under normal conditions, the simulations have been carried out and show that the studied PVPS can operate at its optimum energy, and power quality enhancement is achieved through the integration of a specific harmonic filtering algorithm.

Keywords

photovoltaic power station, PV inverter, reactive power control, harmonic isolation method, specific harmonic compensation, reaching the reactive current limit

1 Introduction

Global population growth and industrial development have increased energy demand. Over the past decade, to mitigate the effects of pollution on the environment, great effort has been concentrated on green energy development, including wind and solar. Grid-connected PV power stations are becoming more popular due to their significant benefits over other PV systems, including cost-effectiveness, low maintenance, and reliability. Compared to off-grid solar PV systems, this type of solar energy system allows for decoupled control of active and reactive power to enhance grid power quality [1, 2]. This is possible because grid-connected PV systems can exchange power with the utility grid, allowing the PV inverter to manage both the real power delivered to the grid and the reactive power injected or absorbed for voltage control and stability. Elsewhere, modern solar energy conversion systems (SECSs), integrating nonlinear loads like power electronics, are controlled to generate active power for the grid and simultaneously improve grid power quality by minimizing harmonic voltage and current distortions using different techniques, such as the installation of passive filters, such as shunt and series filters, and active filtering, which has now become a mature technology for harmonic and reactive power compensation. They also ensure service continuity during any type of fault to maintain grid stability and reliability [3, 4]. Due to their high efficiency, power electronic converters can be used to provide certain auxiliary services (absorption or injection of reactive power to achieve voltage, control and compensation of harmonic currents) [5]. Recently, many researchers have studied how SECS converters, placed between a PV generator and the grid, can improve power quality by mitigating harmonics and addressing voltage fluctuations. In Reference [6], Ibrahim et al. have improved the power quality of a grid-integrated solar PV by attenuating harmonics using a SAF (Shunt Active Filter). In this

Cite this article as: Ouai, A. "Achieving Specific Compensation of Current Harmonics in Grid Connected PV Power Station Under Limited Reactive Current", Periodica Polytechnica Electrical Engineering and Computer Science, 2026. https://doi.org/10.3311/PPee.44126

work, the SAF control is based on d-q theory, while the PV system generates power from the sun and injects it into the grid. In [7], to obtain a high-quality grid voltage waveform, a new technique was proposed for selective voltage harmonics compensation at the CP. Harmonics filtering operation is ensured by controlling the DG (Distributed Generator) interface converters. The PV system presented in [8] is controlled for working in MPPT mode under unbalanced voltage conditions using a fuzzy logic controller, while harmonic mitigation and reactive power compensation are simultaneously achieved through a SAPF. In [9], a new control algorithm for PV system energy management was suggested by Ouai et al., which ensures simultaneous active power production, reactive power control, and grid current harmonics compensation within its power capacity. Moreover, a coordinated system of passive and active filters was used in [10]. The active filter was employed to mitigate the current harmonic distortion from nonlinear loads, while a passive filter was specifically designed to remove the 5^{th} and 7^{th} harmonics. In [11], the PRES compensator is used with an active filter to reduce grid current harmonics in the PV array plant. In addition, the harmonics produced by the DC-DC converter of an off-grid PV system were mitigated by placing an LC filter, which is a type of passive filter [12]. In another study, to suppress unwanted harmonics generated by a nonlinear load connected to a distributed generation system within standard limits, two types of filters (passive and shunt active filter) were employed [13]. In Ref. [14], a PV system is controlled for MPPT production and power quality enhancement using an improved DPC (Direct Power Control) strategy and a SAF. This control strategy uses a PI controller for DC bus voltage regulation, combined with a fuzzy logic MPPT controller. An Adaline algorithm, a type of neural network, is used to identify current harmonics from a modeled nonlinear load. In [15], an LMF (Least Mean Fourth)-based algorithm was used in a solar PV plant to enhance power quality by reducing harmonic distortion in grid currents and voltages, helping the system meet the standards of IEEE-519 [16]. At the last, an LCL filter is used to suppress high-frequency harmonic currents from PV inverters, and this filtering works effectively even under partial shading conditions [17].

In the above cited-papers, the DC-AC PWM converter's capacity, in terms of harmonics compensation of the 5^{th} and 7^{th} predominant harmonic components under limited reactive power, has not yet been evaluated.

This paper presents a new control strategy for a PVPS to achieve both active power generation and simultaneous power quality enhancement. This last is applied to the PV inverter; it allows immediately compensating for reactive power, filtering the 5^{th} and 7^{th} predominant components of the nonlinear load at the CP without reaching the inverter's reactive current limit, if possible. Otherwise, the compensation is canceled, while the PVPS is controlled to achieve an active/reactive power injection with a stable DC voltage.

Simulation results are used to investigate the feasibility and viability of the proposed control strategy for mitigating specific current harmonics. In brief, the main contributions of this paper are as follows:

- A new algorithm is developed for compensating reactive power and filtering the specific harmonic components (the 5^{th} and 7^{th} harmonics) without PV inverter overrating.
- The filtering operation of specific harmonic components is omitted when the reactive current limit is reached due to reactive power injection.
- Validation of the proposed approach's effectiveness through simulation tests performed with and without reaching the reactive current limit.

The paper is structured as follows: The first section reviews the power quality enhancement issue in photovoltaic systems by discussing various control strategies used to mitigate harmonics and address voltage fluctuations, along with the paper's main contributions. The second section presents the detailed configuration of the Hokuto solar station, the reasons for choosing this mega solar plant, and the modeling part and shows the schematic scheme of the proposed PV inverter control for power generation and specific harmonic mitigation. The third section details the proposed harmonic isolation technique based on the HSF. The fourth section discusses the new approach developed to improve the capacity of PV inverter harmonic current compensation. Finally, the fifth section validates the proposed control model through simulation, demonstrating its effectiveness under different operating scenarios.

2 PVPS configuration and operating principle

The PVPS under study is about the second stage 1.2 MW system of the Hokuto solar station, which was installed at the end of 2009. It was selected due to the availability of technical characteristics and its suitability as a model for large-scale PV systems. Fig. 1 represents the system configuration of this mega-solar plant [18].

This research focuses on controlling a LS-PCS (Large Scale-Power Conditioning System) 400 kW PV inverter to enhance the electrical grid power quality. The LS-PCS's

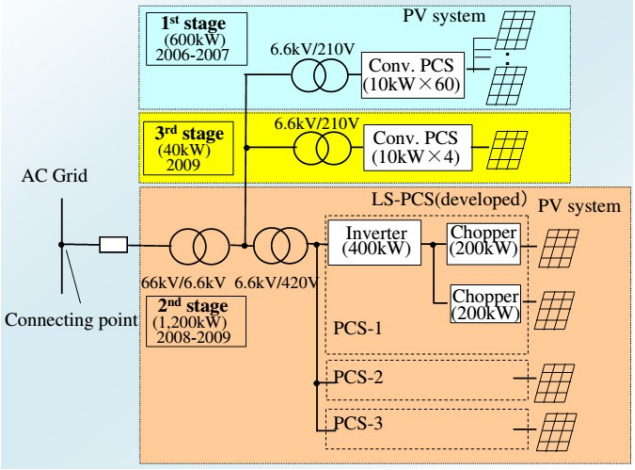


Fig. 1 The studied PVPS configuration [18]

electrical properties and the 400 kW PV inverter are detailed in Table 1 and Table 2, respectively [18, 19].

However, the schematic diagram of the proposed 400 kW PV system, including a nonlinear load, is shown in Fig. 2 and is coupled at the CP.

Table 1 LS-PCS electrical characteristics [20]

Parameter	Value
Output power (S, P)	420 kVA / 400 kW
AC output voltage	420 V ±10%
DC input voltage	230–600 V
Switching frequencies	4–6 kHz
Conversion rate	from 30% to 100%
Control operations	Power optimization Harmonics suppression

Table 2 330TS-SV inverter parameters [21]

Parameter	Value
Dimensions (H × W × D)	200 × 120 × 80 cm
Weight	1200 kg
Max. DC voltage	900 V
Nominal AC power	400 kW
Max. efficiency	98 %
Operating temperature	−20 à +40 °C

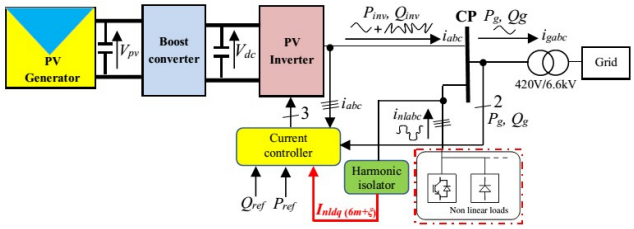


Fig. 2 Proposed PV inverter control scheme for power control and specific harmonic elimination

The voltages of the electrical network's bus bar can be expressed as follows [22]:

$$\begin{cases} v_{ga}(t) = V_m \cos(\omega t) \\ v_{gb}(t) = V_m \cos\left(\omega t + \dfrac{2\pi}{3}\right) \\ v_{gc}(t) = V_m \cos\left(\omega t - \dfrac{2\pi}{3}\right) \end{cases} \quad (1)$$

Where V_m is the maximum phase voltage and ω is the grid angular frequency.

In addition, Eqs. (2) and (3) [23] describe the voltages and currents that result from using the *dq* control.

$$\begin{bmatrix} v_d \\ v_q \end{bmatrix} = \frac{2}{3} \begin{bmatrix} \cos(\omega t) & \cos\left(\omega t - \dfrac{2\pi}{3}\right) & \cos\left(\omega t + \dfrac{2\pi}{3}\right) \\ -\sin(\omega t) & -\sin\left(\omega t - \dfrac{2\pi}{3}\right) & -\sin\left(\omega t - \dfrac{2\pi}{3}\right) \end{bmatrix} \times \begin{bmatrix} v_{ga} \\ v_{gb} \\ v_{gc} \end{bmatrix} \quad (2)$$

$$\begin{bmatrix} i_d \\ i_q \end{bmatrix} = \frac{2}{3} \begin{bmatrix} \cos(\omega t) & \cos\left(\omega t - \dfrac{2\pi}{3}\right) & \cos\left(\omega t + \dfrac{2\pi}{3}\right) \\ -\sin(\omega t) & -\sin\left(\omega t - \dfrac{2\pi}{3}\right) & -\sin\left(\omega t - \dfrac{2\pi}{3}\right) \end{bmatrix} \times \begin{bmatrix} i_{ga} \\ i_{gb} \\ i_{gc} \end{bmatrix} \quad (3)$$

Thus, the powers of the PV system that are provided to the grid are determined by [24] as follows:

$$P_g = \frac{3}{2}\left(v_d i_d + v_q i_q\right), \quad (4)$$

$$Q_g = \frac{3}{2}\left(v_q i_d + v_d i_q\right). \quad (5)$$

From Eqs. (4) and (5) of the PVPS model, the PV inverter control diagram presented in Fig. 3 is directly derived. Proportional integral (PI-1 and PI-2) controllers

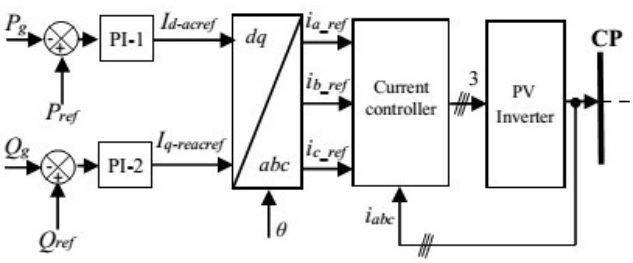


Fig. 3 Control of the PV inverter

have been designed to control active and reactive power levels delivered to the grid.

In this study, to achieve strong filtering capability, modifications must be applied only to the PV inverter-side current controller. A three-phase non-linear current controller known as the "modulated hysteresis current controller" is selected to maintain a fixed IGBT switching frequency.

3 Harmonic isolation technique

Diverse methods exist for extracting harmonic reference currents, which can be principally categorized into time-based and frequency-based techniques [23].

3.1 Highly selective filter

An HSF, which is a filter suitable for precisely extracting on the (α–β) axes the specific harmonic to be mitigated from other frequencies. The HSF is defined by the following general equation [23]:

$$H(s)=\frac{\hat{x}_{\alpha\beta}(s)}{x_{\alpha\beta}(s)}=k\frac{(s+k)+j.\omega_c}{(s+k)^2+j.\omega_c^2}, \tag{6}$$

where $x_{\alpha\beta}$ term of the analyzed signal is provided by:

$$x_{\alpha\beta}(s)=x_\alpha(s)+j.x_\beta(s). \tag{7}$$

Additionally, $\hat{x}_{\alpha\beta(s)}$ represents the (α–β) filtered component, which is determined by:

$$\hat{x}_{\alpha\beta}(s)=\hat{x}_\alpha(s)+j\times\hat{x}_\beta(s). \tag{8}$$

Notice that, for $s=j.\omega_c$, the module of $H(s)=1$, corresponding to a gain of 0 dB while the phase shift is zero. According to Eqs. (6)–(8), it can be shown that $x_{\alpha(s)}$ and $\hat{x}_{\beta(s)}$ are [25]:

$$\hat{x}_\alpha(s)=\frac{k}{s}\left[x_\infty(s)-\hat{x}_\alpha(s)\right]-\frac{\omega_c}{s}\hat{x}_\beta(s) \tag{9}$$

$$\hat{x}_\beta(s)=\frac{k}{s}\left[x_\beta(s)-\hat{x}_\beta(s)\right]-\frac{\omega_c}{s}\hat{x}_\alpha(s) \tag{10}$$

Fig. 4 shows the block diagram of the HSF tuned to the ω_c pulsation [26]. This filter operates similarly to a second-order tuned oscillator.

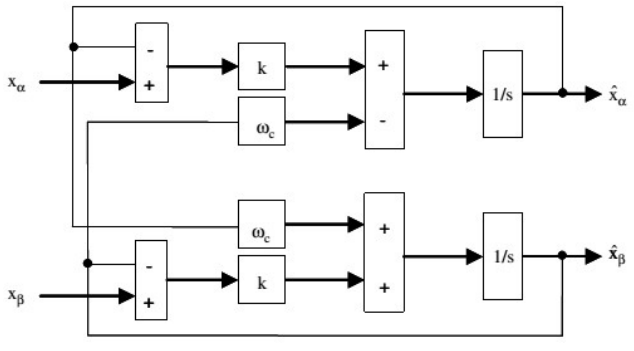


Fig. 4 The ω_c pulse-tuned HSF

The three-phase nonlinear load currents (i_{nla}, i_{nlb} and i_{nlc}) are transformed using the Clarke transformation function in the suggested harmonic isolation technique. As a result, the two-phase nonlinear load currents ($i_{nl\alpha}$ $i_{nl\beta}$) are converted as follows [27]:

$$\begin{bmatrix} i_{nl\alpha} \\ i_{nl\beta} \end{bmatrix}=\sqrt{\frac{2}{3}}.\begin{bmatrix} 1 & -\frac{1}{2} & -\frac{1}{2} \\ 0 & \sqrt{\frac{3}{2}} & -\sqrt{\frac{3}{2}} \end{bmatrix}\begin{bmatrix} i_{nla} \\ i_{nlb} \\ i_{nlc} \end{bmatrix}. \tag{11}$$

The principal benefit of the examined HSF is that it directly draws the first harmonic or a specific order harmonic of a current from the following equations define the (α–β) axes:

$$\hat{i}_{nl\alpha}(s)=\frac{k}{s}\left[i_{nl\alpha}(s)-\hat{i}_{nla}(s)\right]-\frac{\omega_c}{s}\hat{i}_{nl\beta}(s), \tag{12}$$

$$\hat{i}_{nl\beta}(s)=\frac{k}{s}\left[i_{nl\beta}(s)-\hat{i}_{nla}(s)\right]-\frac{\omega_c}{s}\hat{i}_{nl\alpha}(s). \tag{13}$$

Observe that $\hat{i}_{nl\alpha}$ and $\hat{i}_{nl\beta}$ in Eqs. (12) and (13) might represent either the fundamental harmonic or a specific harmonic element of the current.

At last, the two-phase currents ($\hat{i}_{nl\alpha}$ and $\hat{i}_{nl\beta}$) in the (d–q) reference frame are expressed using the Park Transformation (PT) as follows:

$$\begin{bmatrix} \hat{i}_{nld} \\ \hat{i}_{nlq} \end{bmatrix}=\begin{bmatrix} \cos(\theta) & \sin(\theta) \\ -\sin(\theta) & \cos(\theta) \end{bmatrix}\begin{bmatrix} \hat{i}_{nl\alpha} \\ \hat{i}_{nl\beta} \end{bmatrix} \tag{14}$$

3.2 Specific harmonic elimination strategy

The polluting currents include direct and reverse harmonics of the (6 m ± 1) order, which are 5, 7, 11, and 13. Indeed, HSF provides the following expression [23] for the $\alpha\beta$ components of a specific harmonic of order ($6m+\xi$):

$$\begin{cases} i_{nl\alpha(6m+\zeta)}(s)=\frac{k}{s}\left[i_{nl\alpha}(s)-i_{nl\alpha(6m+\zeta)}(s)\right]- \\ -\zeta\frac{\omega_{c(6m+\zeta)}}{s}i_{nl\beta(6m+\zeta)}(s) \\ i_{nl\beta(6m+\zeta)}(s)=\frac{k}{s}\left[i_{nl\beta}(s)-i_{nl\beta(6m+\zeta)}(s)\right]- \\ -\zeta\frac{\omega_{c(6m+\zeta)}}{s}i_{nl\alpha(6m+\zeta)}(s) \end{cases} \tag{15}$$

From Eq. (15), the HSF parameters can be defined as follows:

- m: Positive integer, m=1,2,3,….
- k: Gain of HSF.
- $\omega_c(6m+\xi)$: Angular frequency of the specific harmonic to be extracted (5th or 7th)

In our study, the 5th and 7th harmonics are both identified simultaneously. Fig. 5 clearly shows the identification diagram of the 5th and 7th harmonic currents based on the HSF.

4 A new control strategy for improving PV inverter harmonic currents compensation capacity

The PVPS's power capacity depends on its current limit I_{LMT} that can be determined by the following expression:

$$I_{LMT} = \sqrt{2}\frac{P_{LMT}^2 + Q_{LMT}^2}{3V_{CP}}. \quad (16)$$

Where P_{LMT} and Q_{LMT} represent the real and reactive power limits for a given working point. Therefore, Eq. (17) is used to compute the limit value of reactive current that can be used for reactive power and harmonic currents compensation:

$$I_{q-reacrefLMT} = \sqrt{I_{LMT} - I_{d-acrefLMT}}. \quad (17)$$

In order to modify the PV inverter control for enhancing the grid power quality by filtering the specific harmonics of the 5th and 7th with no over-rating, it is suggested in this research paper to provide the new resulting references I_{d-ref} and I_{q-ref} for real power generation, reactive power injection, and harmonics filtering by using the following proposed approach:

First case, if the reactive power current reference $I_{q-reacref}$ verifies:

$$I_{q-reacref} \geq I_{q-reacrefLMT}. \quad (18)$$

In this case, the PV inverter is exceeding its limit for reactive power compensation; it can only compensate a portion of the required reactive power and therefore the resulting references I_{d-ref} and I_{q-ref} become:

$$\begin{cases} I_{d-ref} = I_{d-acref} \\ I_{q-ref} = \pm I_{q-reacrefLMT} \end{cases}. \quad (19)$$

Second case, if Iq-reacref verifies:

$$I_{q-reacref} < I_{q-reacrefLMT}. \quad (20)$$

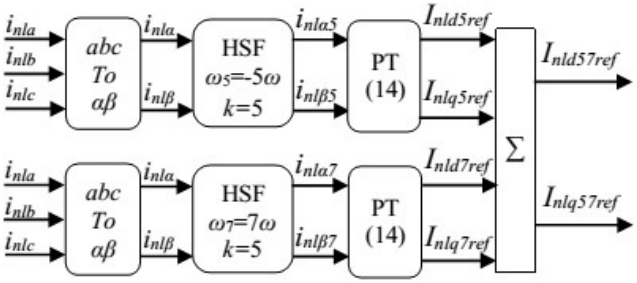


Fig. 5 Identification of the 5th and 7th harmonics *d-q* references using HSF

This indicates that a part of the reactive current is disponible, it could be utilized for harmonic filtering operations. The proposed specific harmonic compensation strategy aims to compensate instantaneously for the entirety of the 5th and the 7th predominant harmonic components, if it is feasible. If not, the harmonic compensation operation is cancelled. In the following, the details of the solution scenarios:

The first scenario occurs if:

$$\sqrt{\left(I_{d-acref} + I_{nld57ref}\right)^2 + \left(I_{q-reacref} + I_{nld57ref}\right)^2} \leq I_{LMT}. \quad (21)$$

Under this circumstance, the PV inverter is able to compensate the required reactive power and filter the entire 5th and 7th dominant harmonic components.

As a result, the total current references of the whole control system, I_{d-ref} and I_{q-ref} can be written as:

$$\begin{cases} I_{d-ref} = I_{d-acref} + I_{nld57ref} \\ I_{q-ref} = I_{q-reacref} + I_{nlq57ref} \end{cases}. \quad (22)$$

In the second scenario, we have:

$$\sqrt{\left(I_{d-acref} + I_{nld57ref}\right)^2 + \left(I_{q-reacref} + I_{nld57ref}\right)^2} > I_{LMT}. \quad (23)$$

According to last inequality, it is clear that both 5th and 7th harmonics cannot be compensated without avoiding excessive PV inverter over-rating.

Consequently, the specific harmonic elimination process is canceled. And the Eq. (22) can be simplified as:

$$\begin{cases} I_{d-ref} = I_{d-acref} \\ I_{q-ref} = I_{q-reacref} \end{cases}. \quad (24)$$

Fig. 6 illustrates the modified block diagram for the proposed PV inverter control technique. It displays the adjusted version of Fig. 2.

The new specific filtering references $I_{nld57ref}$ and $I_{nlq57ref}$ are shown in bold red.

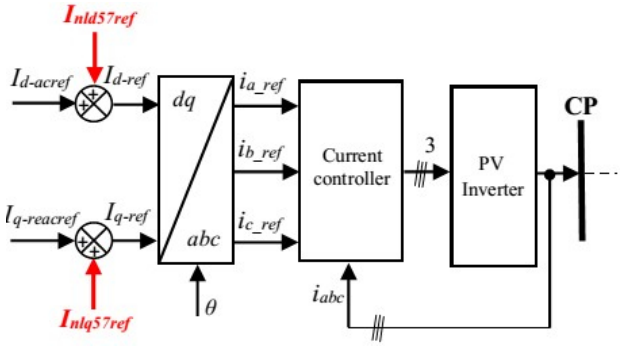


Fig. 6 Modified PV inverter control containing specific harmonic mitigation

5 Simulation results

The simulation tests were performed in the MATLAB environment [28]. The suggested control approach is tested for a 400 kW LS-PCS under different operating conditions, whose electrical parameters are shown in Table 1.

To improve filter selectivity and dynamic performance, k was selected to be 5 for the two HSFs employed for the isolation of the specific harmonic currents (the 5th and 7th), see section 3. 2. The switching frequency f_s is set as 5 kHz for the hysteresis current controllers of the PV inverter.

The whole load powered by the studied PVPS is a diode-rectifier non-linear load circuit with an inductive-resistive load. Table 3 defines the parameters of our simulation study.

5.1 Reactive power and specific harmonic components compensation without reaching the reactive current limit

In the first section, reactive power control and filtering the whole specific high-order harmonics (the 5th and 7th harmonics) without exceeding the reactive current limit $I_{q-reacrefLMT}$ are examined.

In this simulation, a 38 kVar reactive power compensation and an injection of 200 kW active power are considered (P_{ref}=200 kW, Q_{ref}=38 kVar, Q/P=0.19), as shown in Fig. 7(a).

It should be noted that the reactive power limit value can be utilized to compensate reactive power and harmonic currents is about 170 kVar (Q_{LMT}=170 kVar), as mentioned in Table 3.

Fig. 7(b) shows the current waveform of the considered non-linear load $i_{nla}(t)$ of 100 kW connected at PC, and its calculated value of THD is about 30.58%, as shown in Fig. 7(c).

The waveforms of the grid current i_{ga}(t) at PC with and without a specific harmonic filtering strategy are shown in Fig. 7(d) and Fig. 8(a), respectively.

Table 3 Parameters used in simulation study

Parameter	Value
Grid	U_n=420 V (line to line)
	f = 60 Hz, ω= 376.8 rad/s
PV inverter	V_{dc} = 600 V
	f_s = 5 kHz
	P = 400 kW, Q =220 kVar
HSF gain	k =5
Harmonics considered	5th and 7th
Working point power limits	P_{LMT} =200 kW
	Q_{LMT} =170 kVar
Nonlinear load	100 kW

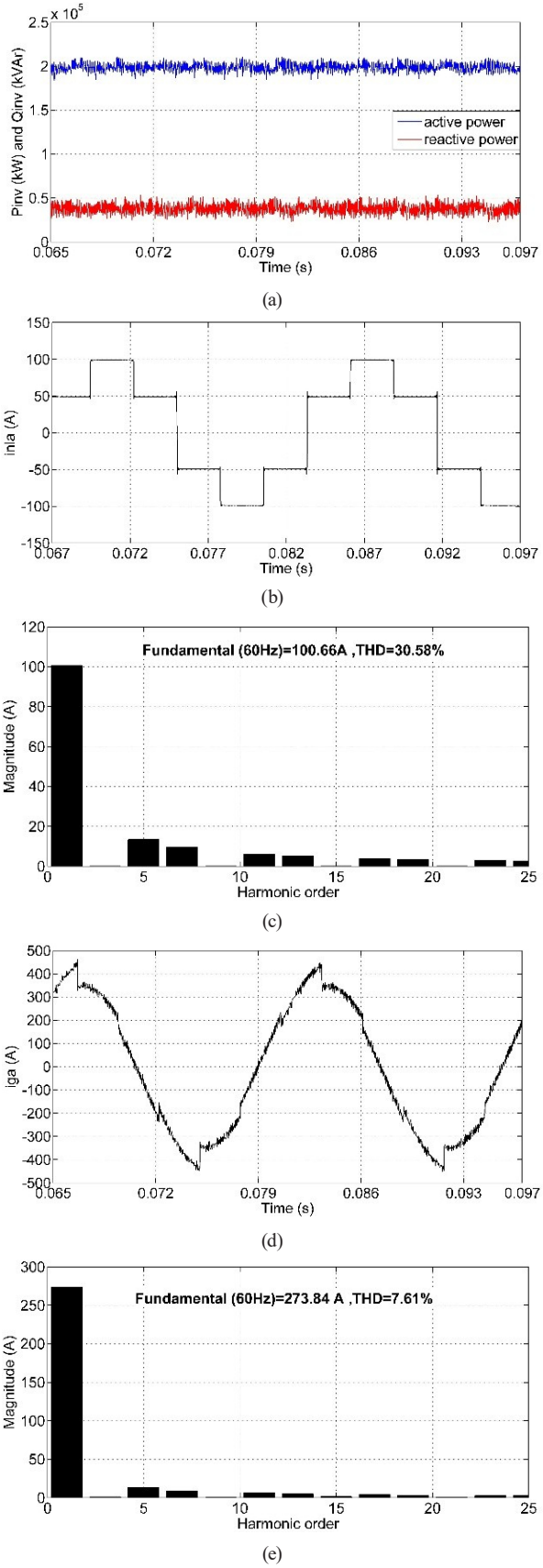


Fig. 7 Simulation results without the proposed specific harmonic filtering strategy: (a) Active and reactive power injection; (b) Non-linear load current $i_{nla}(t)$; (c) THD of $i_{nla}(t)$; (d) Waveform of grid current $i_{ga}(t)$; (e) THD of $i_{ga}(t)$

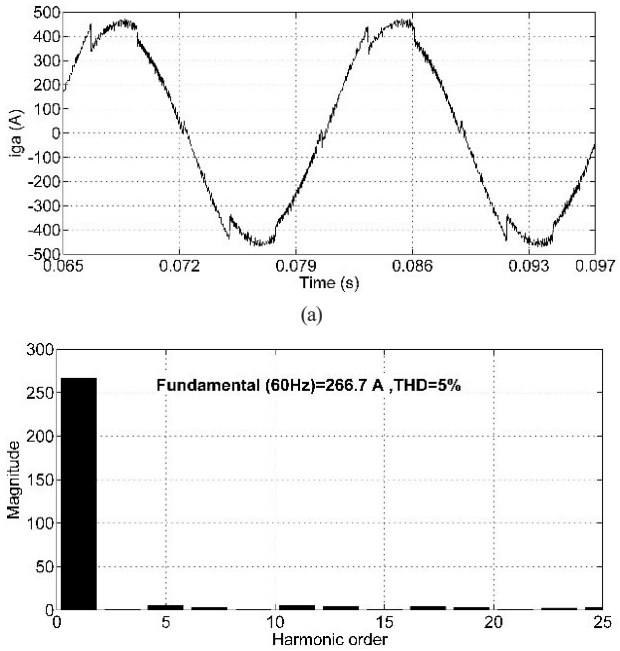


Fig. 8 Simulation results with the proposed specific harmonic filtering strategy: (a) Waveform of grid current $i_{ga}(t)$; (b) THD of $i_{ga}(t)$

The performance of the proposed approach is evaluated though THD analysis. It proves that the grid current THD is reduced from 7.61 to 5%, as shown in Figs. 7(e) and 8(b).

As a result, the RMS values for the 5th and 7th dominating harmonic currents have decreased from approximately 0.71 A to 0.24 A and from 0.46 A to 0.32 A, respectively.

Also, one can notice that the harmonic currents RMS of the other ranks (like the 11th, 13th, 17th, or 19th) remain unchanged after compensation.

In this case, the PV inverter performs reactive power compensation and filters the most dominant 5th and 7th harmonic components.

5.2 Reactive power and specific harmonic components compensation under a reached reactive current limit

5.2.1 Reaching the reactive current limit under reactive power injection

In this case, the PVPS is required to compensate a reactive PV inverter power reference of 250 kVar and to filter the 5th and 7th harmonic components.

Figs. 9 and 10 illustrate the obtained simulation analysis results with and without specific harmonic current compensation.

Under this operating condition, the reactive current limit $I_{q-reacrefLMT}$ is saturated for only reactive power injection (250 kVar > Q_{LMT}).

Then, the PV inverter is controlled to inject 200 kW of active power and compensate only 170 kVar from 250 kVar.

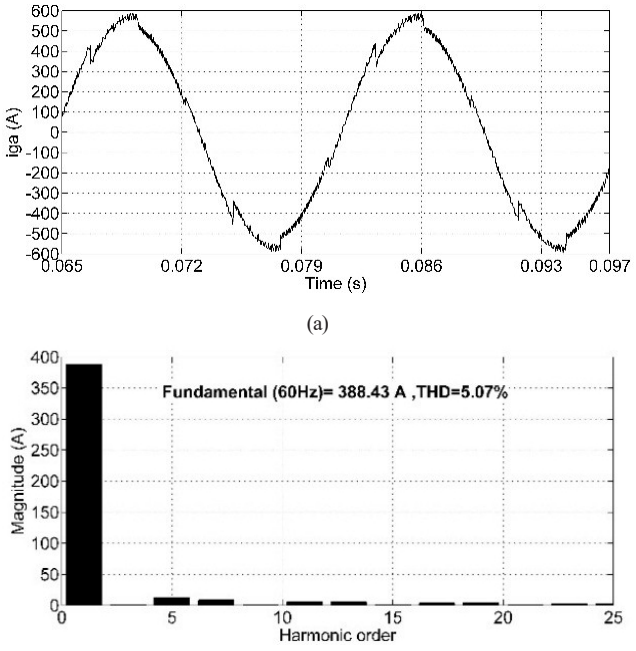


Fig. 9 Simulation results without the proposed specific harmonic filtering strategy under a reached reactive current limit due to reactive power compensation: (a) Waveform of grid current $i_{ga}(t)$; (b) THD of $i_{ga}(t)$

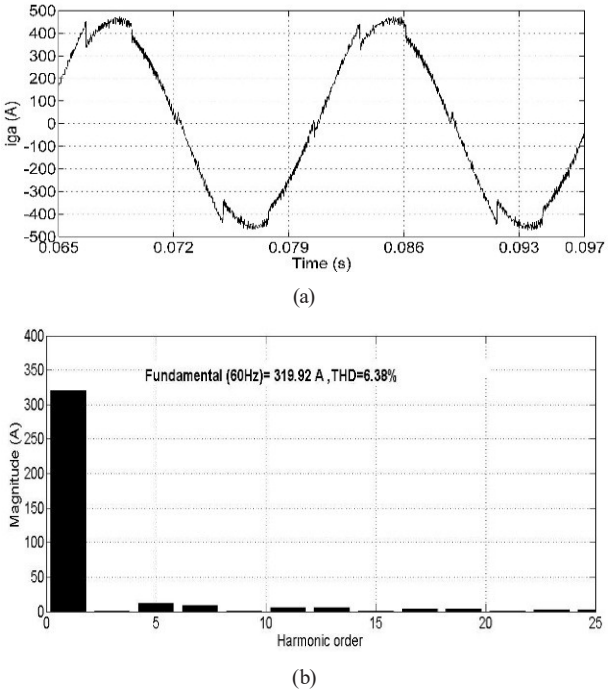


Fig. 10 Simulation results with the proposed specific harmonic filtering strategy under a reached reactive current limit due to reactive power compensation: (a) Waveform of grid current $i_{ga}(t)$; (b) THD of $i_{ga}(t)$

Therefore, there is no compensation of the harmonic currents injected by the nonlinear load.

After the harmonic filtering operation, as can be observed from Fig. 10(a), the grid current becomes more distorted if compared with its pre-filtering waveform (Fig. 9(a)).

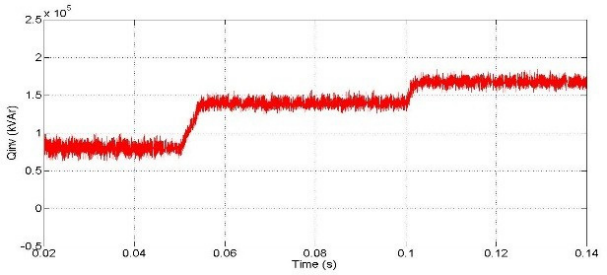
According to grid current FFT analysis, as shown in Figs. 9(b) and 10(b), after compensation the fundamental component value of the grid current is reduced from 388.43 A to 319.92 A, and consequently the THD level is increased from around 5.07% to 6.38%.

5.2.2 Reaching the reactive current limit under specific harmonic components filtering

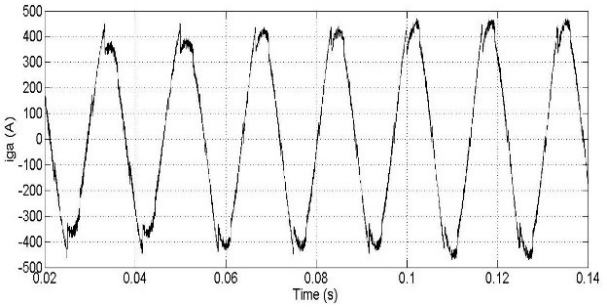
As mentioned before (see Section 4), the reactive current command can be reached due to the harmonic suppression current command.

This situation of current command saturation is studied in the following section.

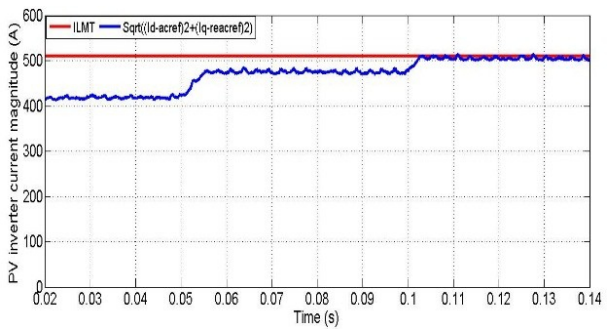
In this test, the active power reference, P_{ref}, is always set to 200 kW while different step changes in the reactive power reference Q_{ref} are applied, as shown in Fig. 11(a).



(a)



(b)



(c)

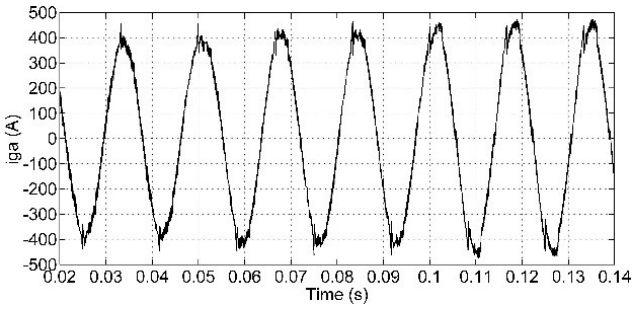
Fig. 11 Simulation results without the proposed specific harmonic filtering strategy under a reached reactive current limit due to harmonic components filtering: (a) Different step changes in the reactive power Q; (b) Waveform of grid current $i_{ga}(t)$; (c) PV inverter current command

At t=0.05 s, the reactive power at the output of the PV inverter is stepped from 80 kVar to 140 kVar and from 140 kVar to 168 kVar at t=0.1 s.

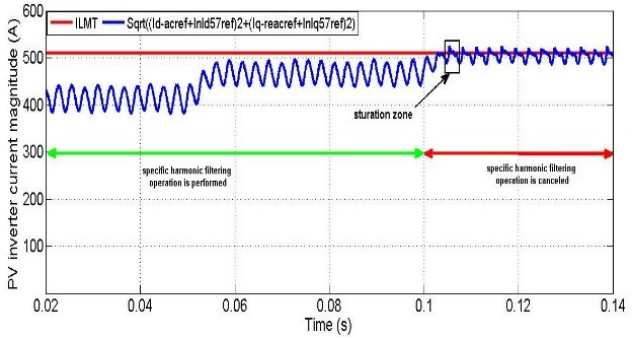
In addition, the grid current $i_{ga}(t)$ waveform and the PV inverter current command response for different values of reactive power should be injected into the grid without harmonic current compensation are shown in Figs. 11(b) and (c) respectively.

With PV inverter specific harmonic compensation, for t<0.1, the grid current quality is improved by compensating the reactive power and filtering the main current harmonics (the 5th and 7th) as can be observed in Fig. 12(a).

But, where Q_{ref}=168 kVar is performed at t=0.1 s, reactive power injection is achieved because it is below the maximum (170 kVar). Therefore, there are 2 kVar that may be exploited for active harmonic filtering. This fraction is not sufficient to suppress both 5th and 7th harmonics, so the PV inverter current command reaches the saturated zone, as shown in Fig. 12(b). Based on this analysis, from t=0.1 s, it is evident that specific compensation of current harmonics is cancelled and PV inverter current commands are decreased to (I_{d-ref}=$I_{d-acref}$ and I_{q-ref}=$I_{q-reacref}$) for only active and reactive power injection.



(a)



(b)

Fig. 12 Simulation results with the proposed specific harmonic filtering strategy under a reached reactive current limit due to harmonic components filtering: (a) Waveform of grid current $i_{ga}(t)$; (b) PV inverter current command

6 Conclusion

This paper has proposed a novel approach for power quality enhancement of a grid-connected PV power station. The study's objective is to instantaneously suppress the 5th and 7th most significant harmonic currents; if this is not possible, the filtering process is canceled. However, the PV inverter is controlled to achieve active and reactive power injection and to improve the capacity of active harmonic current compensation without reaching the reactive current limit. Firstly, the block diagram of PV inverter active/reactive power injection control has been presented. Then, we focused particularly on a specific harmonic compensation strategy. To improve filtering, an HSF is used to isolate the 5th and the 7th predominant harmonic components. The performance and the effectiveness of the suggested control for specific harmonic compensation are examined and verified through different scenarios. The grid current's THD was calculated via FFT analysis under both scenarios: where the reactive current limit was reached and where it was not. This calculation was performed at various operating points, determined by different levels of reactive power injection, both before and after a specific harmonic current compensation was applied.

References

[1] Mombekova, G., Nurgabylov, M., Baimbetova, A., Keneshbayev, B., Izatullayeva, B. "The Relationship Between Energy Consumption, Population and Economic Growth in Developing Countries", International Journal of Energy Economics and Policy, 14(3), pp. 368–374, 2024. https://doi.org/10.32479/ijeep.15614

[2] Bamisile, O., Acen, C., Cai, D., Huang, Q., Staffell, I. "The environmental factors affecting solar photovoltaic output", Renewable and Sustainable Energy Reviews, 208, 115073, 2025. https://doi.org/10.1016/j.rser.2024.115073

[3] Hossain, M. K., Chowdhury, P., Nowshin, I., Islam, M. R., Al-Hysam, A., Farrok, O. "Grid-connected inverter for photovoltaic energy harvesting: Advances in topologies and control techniques", Energy Conversion and Management: X, 29, 101422, 2026. https://doi.org/10.1016/j.ecmx.2025.101422

[4] Rahman, S., Saha, S., Islam, S. N., Arif, M. T., Mosadeghy, M., Haque, M. E. "Analysis of Power Grid Voltage Stability with High Penetration of Solar PV Systems", IEEE Transactions on Industry Applications, 57(3), pp. 2245–2257, 2021. https://doi.org/10.1109/TIA.2021.3066326

[5] Sabo, A., Suleiman, H. O., Dahiru, Y., Bukar, B., Emmanuel, A., Kamaldeen, R. O. "The Role of Power Electronic Converters in Microgrid Technology: A Review of Challenges, Solutions, and Research Directions", European Journal of Theoretical and Applied Sciences, 2(2), pp. 799–808, 2024. https://doi.org/10.59324/ejtas.2024.2(2).71

[6] Ibrahim, Z., Abu Hassim, A. S., Talib, M. H. N., Mat Lazi, J., Isa, S. N. B. M., Mustafa, R. "Performance investigations of photovoltaic grid connection for shunt active power filter with different PWM generation", Journal of Theoretical and Applied Information Technology, 57(2), pp. 305–312, 2013.

[7] Savaghebi, M., Vasquez, J. C., Jalilian, A., Guerrero, J. M., Lee, T.-L. "Selective compensation of voltage harmonics in grid-connected microgrids", Mathematics and Computers in Simulation, 91, pp. 211–228, 2013. https://doi.org/10.1016/j.matcom.2012.05.015

[8] Sreerami Reddy, N., Hameed, S. K. "Fuzzy Based Current Harmonic Suppression and Reactive Power Compensation in a Grid Connected PV System Using Shunt Active Filter", International Journal of Science and Research, 4(5), pp. 2102–2107, 2015. https://dx.doi.org/10.21275/SUB154584

[9] Ouai, A., Mokrani, L., Machmoum, M., Houari, A. "Control and energy management of a large-scale grid-connected PV system for power quality improvement", Solar Energy, 171, pp. 893–906, 2018. https://doi.org/10.1016/j.solener.2018.06.106

[10] Smadi, A. A., Lei, H., Johnson, B. K. "Distribution System Harmonic Mitigation Using a PV System with Hybrid Active Filter Features", In: 2019 North American Power Symposium (NAPS), Wichita, KS, USA, 2019, pp. 1–6. ISBN 978-1-7281-0408-9 https://doi.org/10.1109/NAPS46351.2019.9000238

[11] Yadav, U., Gupta, A. "Current Harmonic Mitigation in Grid-Tied Solar Photovoltaic System via PRES", In: 2020 5th IEEE International Conference on Recent Advances and Innovations in Engineering (ICRAIE), Jaipur, India, 2020, pp. 1–5. ISBN 978-1-7281-8868-3 https://doi.org/10.1109/ICRAIE51050.2020.9358290

[12] Adak, S. "Harmonics Mitigation of Stand-Alone Photovoltaic System Using LC Passive Filter", Journal of Electrical Engineering & Technology, 16(5), pp. 2389–2396, 2021. https://doi.org/10.1007/s42835-021-00777-7

[13] Sulibhavi Vishwanath, A., Ankaliki, S. G. "Harmonic Analysis of Non-Linear Loads in Distribution System and Mitigation Using Passive Filters", International Research Journal of Engineering and Technology, 9(5), pp. 1508–1515, 2022.

[14] Boudechiche, G., Aissa, O., Sarra, M., Hatti, M., Belkhiri, S., Mellit, A., Belmili, H., Seddik, B. "Study and Simulation of SAPF Interconnected to a PV System Based on DPC with Disturbance Rejection Principle", In: Proceedings of the 1st International Conference on Advanced Renewable Energy Systems, Tipaza, Algeria, 2022, pp. 21–29. ISBN 978-981-99-2776-0 https://doi.org/10.1007/978-981-99-2777-7_3

[15] Jha, K., Shaik, A. G. "Modified LMF Adaptive Control of Weak AC Grid with High Penetration of Solar Energy", In: 2023 IEEE International Conference on Advanced Systems and Emergent Technologies (IC_ASET), Hammamet, Tunisia, 2023, pp. 21–29. ISBN 979-8-3503-2103-6 https://doi.org/10.1109/IC_ASET58101.2023.10150936

[16] IEEE "519-2014 - IEEE Recommended Practice and Requirements for Harmonic Control in Electric Power Systems", IEEE, New York, USA, 2014.
https://doi.org/10.1109/IEEESTD.2014.6826459

[17] Ouai, A., Köten, H., Mokrani, L., Machmoum, M. "VSC Control in Grid-Connected PV Plant for Power Generation and Harmonics Mitigation During Partial Shading Irradiance Condition", In: 2024 IEEE 4th New Energy and Energy Storage System Control Summit Forum (NEESSC), Hohhot, China, 2024, pp. 200–204. ISBN 979-8-3503-8902-9
https://doi.org/10.1109/NEESSC62857.2024.10733423

[18] Konishi, H. "Study of MPPT Control Method for Large-Scale Power Conditioning System in Hokuto Mega-Solar System", Journal of International Council on Electrical Engineering, 4(2), pp. 173–178, 2014.
https://doi.org/10.5370/JICEE.2014.4.2.173

[19] Ouai, A., Mokrani, L., Machmoum, M., Houari, A. "Power Quality Improvement of a Solar Energy Conversion System by a Coordinated Active and LCL Filtering", Periodica Polytechnica Electrical Engineering and Computer Science, 65(4), pp. 373–381, 2021.
https://doi.org/10.3311/PPee.17215

[20] Konishi, H., Iwato, T., Kudou, M. "Verification test results of 2nd stage in Hokuto mega-solar system", In: 2011 37th IEEE Photovoltaic Specialists Conference (PVSC), Seattle, WA, USA, 2011, pp. 2375–2379. ISBN 978-1-4244-9966-3
https://doi.org/10.1109/PVSC.2011.6186428

[21] Ouai, A., Mokrani, L., Machmoum, M. "Control of a 400 kW Grid-Connected PV Array with and without MPPT Algorithm", In: 2024 12th International Conference on Systems and Control (ICSC), Batna, Algeria, 2024, pp. 132–136. ISBN 979-8-3315-3182-9
https://doi.org/10.1109/ICSC63929.2024.10928883

[22] Ouai, A., Mokrani, L., Machmoum, M., Houari, A. "Voltage Error Estimation-Based Fault Diagnosis Method for Three-phase PWM-inverter in Grid-connected Photovoltaic Power System without any Over-rating", Periodica Polytechnica Electrical Engineering and Computer Science, 68(3), pp. 232–239, 2024.
https://doi.org/10.3311/PPee.23416

[23] Gaillard, A., Poure, P., Saadate, S., Machmoum, M. "Variable speed DFIG wind energy system for power generation and harmonic current mitigation", Renewable Energy, 34(6), pp. 1545–1553, 2009.
https://doi.org/10.1016/j.renene.2008.11.002

[24] Ouai, A., Mebarek, A. R., Mokrani, L., Shahnia, F. "An Efficient Active Filtering Strategy for Reducing Total Harmonic Distortion in High-Penetration Gridconnected Solar PV System", In: 2025 IEE 5th New Energy and Energy Storage System Control Summit Forum (NEESSC), Hohhot, China, 2025, pp. 171–175. ISBN 979-8-3315-0123-5
https://doi.org/10.1109/NEESSC66038.2025.11199676

[25] Shu, Z., Lin, H., Ziwei, Z., Yin, X., Zhou, Q. "Specific order harmonics compensation algorithm and digital implementation for multi-level active power filter", IET Power Electronics, 10(5), pp. 525–535, 2017.
http://dx.doi.org/10.1049/iet-pel.2016.0315

[26] Mesbahi, N., Ouari, A., Ould Abdeslam, D., Djamah, T., Omeiri, A. "Direct power control of shunt active filter using high selectivity filter (HSF) under distorted or unbalanced conditions", Electric Power Systems Research, 108, pp. 113–123, 2014.
https://doi.org/10.1016/j.epsr.2013.11.006

[27] Patnaik, S. S., Panda, A. K. "Power quality enhancement using a novel SAPF control scheme employing high selectivity filter", International Journal of Emerging Electric Power Systems, 25(3), pp. 367–381, 2024.
https://doi.org/10.1515/ijeeps-2022-0380

[28] MathWorks "Mathlab (26.1)" [computer program] Available at: https://www.mathworks.com/products/matlab.html [Accessed: 20 March 2026]